Scientia Iranica D (2021) 28(3), 1592–1605

Sharif University of Technology
Scientia Iranica
Transactions D: Computer Science & Engineering and Electrical Engineering
http://scientiairanica.sharif.edu

Tele-operation of autonomous vehicles over additive white Gaussian noise channel

A. Parsa and A. Farhadi*

Department of Electrical Engineering, Sharif University of Technology, Tehran, Iran.

Received 17 September 2019; received in revised form 21 January 2020; accepted 14 April 2020

KEYWORDS
Networked control system;
Tele-operation system;
The describing function;
The unicycle model;
AWGN channel.

Abstract. This paper is concerned with the tele-operation of autonomous vehicles over analog Additive White Gaussian Noise (AWGN) channel, which is subject to transmission noise and power constraint. The nonlinear dynamic of autonomous vehicles is described by the unicycle model and is cascaded with a bandpass filter acting as encoder. Using the describing function method, the nonlinear dynamic of autonomous vehicles is represented by an approximate linear system. Then, the available results for linear control over analog AWGN channel are extended to account for linear continuous time systems with non-real valued and multiple real valued eigenvalues and for tracking a non-zero reference signal. Subsequently, by applying the extended results on the describing function of autonomous vehicles, a mean square control technique including an encoder, a decoder, and a controller is presented for reference tracking of the tele-operation of autonomous vehicles over AWGN channel. The satisfactory performance of the proposed control technique is illustrated by computer simulations.

1. Introduction

1.1. Motivation and background

Tele-operation of autonomous vehicles has become an active research direction in recent years. In these systems, the remote autonomous vehicle must track a reference signal generated by a remote operator which is communicated to it via a wireless link. In this application, the measurements from on-board sensors are also communicated to remote operators to help operator to generate a desired reference signal. One of the abstract models for wireless communication is Additive White Gaussian Noise (AWGN) channel. This channel is an abstract model for satellite communication, deep space communication, and when the line of sight is strong. Therefore, in these situations, we deal with the tele-operation of system given in Figure 1. Very often, autonomous vehicles are battery powered and hence, communication from these vehicles to the base station where the operator is located must be done with minimum possible transmission power to increase the on-board battery life time. Therefore, communication from vehicle to remote controller is subject to noise and power constraint. However, as the communication from the base station to remote vehicle can be done with high transmission power, in the block diagram of Figure 1, the communication link from remote controller to the remote vehicle (dynamic system) can be considered without imperfections and limitations.

The tele-operation of Figure 1 is an example of networked control systems. In networked control systems, we deal with controlling dynamic systems over communication channels subject to imperfections and limitations. Some results addressing basic problems in stability and/or state tracking of dynamic systems over communication channels subject to imperfections and limitations can be found in [1–28]. Dynamic systems

*. *Corresponding author.*
E-mail address: afarhadi@sharif.edu (A. Farhadi)

doi: 10.24200/sci.2020.54447.3755

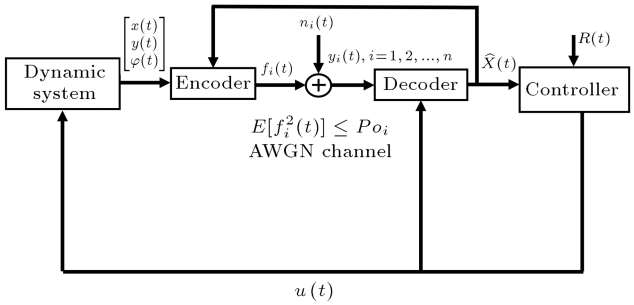

Figure 1. A dynamic system over Multi-Input Multi-Output (MIMO) parallel Additive White Gaussian Noise (AWGN) channel.

can be viewed as continuous alphabet information sources with memory. Therefore, many works in the literature (e.g., [1,12,13,18,19,22–28]) are dedicated to the question of state tracking and/or stability over AWGN channel, which itself is naturally a continuous alphabet channel. Researchers [12,13] addressed the problem of mean square stability and state tracking of linear Gaussian dynamic systems over AWGN channel when noiseless feedback channel was available full time and the communication of control signal from remote controller to system was perfect (see Figure 1). In [12], the authors presented an optimal control technique for asymptotic bounded mean square stability of partially observed discrete time linear Gaussian systems over AWGN channel. In [13], the authors addressed a continuous time version of the problem addressed in [12]. In [22], the researchers considered a framework for discussing control over a communication channel based on Signal-to-Noise Ratio (SNR) constraints and focused particularly on the feedback stabilization of an open loop unstable plant via a channel with a SNR constraint. By examining the simple case of a Linear Time Invariant (LTI) plant and an AWGN channel, the authors in [22] derived necessary and sufficient conditions on the SNR for feedback stabilization with an LTI controller. In [23], the authors addressed the problem of state tracking of nonlinear systems over AWGN channel. In [25], the authors presented a sub-optimal decentralized control technique for bounded mean square stability of a large-scale system with cascaded clusters of sub-systems. Each sub-system is linear and time-invariant and both sub-system and its measurement are subject to Gaussian noise. The control signals are exchanged between sub-systems without any imperfections, but the measurements are exchanged via an AWGN communication network. In [27], the author presented a sub- optimal technique for mean square stability of a distributed system with geographically separated Gaussian sub-systems interconnected by a AWGN communication network. In [28], the authors investigated stabilization and performance issues for MIMO LTI networked feedback systems, in which the Multi-Input Multi-Output (MIMO) communication link is modeled as a parallel noisy Additive White Noise (AWN) channel. The idea of using the describing function for controlling nonlinear dynamic systems over AWGN channel for the first time was presented in [29]. In addition to the AWGN channel, other communication channels, which have caught the attention of networked control systems research community, are the real and the packet erasure channels that are abstract models for communication via the Internet and WiFi links. Other researchers [30] addressed the problems of optimal control and stability of LTI systems over the real erasure channel, which is subject to random packet dropout, where both remote and local controllers operate on the system. Moreover, the problem of optimal control of LTI systems by a remote controller over the real erasure channel was addressed in [31].

The above literature review reveals that the available results on the stability and state tracking of dynamic systems over AWGN channel are mainly concerned with linear dynamic systems. To the best of our knowledge, control of nonlinear dynamic systems over AWGN channel is limited to [23] and [29], which are not concerned with the tele-operation of autonomous vehicles subject to communication imperfections. In the tele-operation of autonomous vehicles, we deal with state tracking as well as reference tracking of nonlinear systems. The dynamic of autonomous vehicles (autonomous underwater, unmanned aerial, and autonomous road vehicles) is described by the six-degree-of-freedom model. However, the vehicle dynamic is handled by an on-board control loop that results in a kinematic unicycle model, which is nonlinear [16]. In addition, in deep space tele-operation systems or when the line of sight is strong, AWGN channel is a suitable model for wireless communication. These issues motivate research on tele-operation of the unicycle model over AWGN channel, which is the subject of this paper.

1.2. Paper contributions

Key contributions of this paper compared to the aforementioned literature are summarized as follows:

1. In the field of nonlinear dynamic systems, the describing function is used for building oscillators [32]. However, in this paper, for the first time, it has been used to stabilize and control a practical nonlinear dynamic system. That is, the unicycle model is an abstract model for describing the dynamics of autonomous underwater, unmanned aerial and autonomous road vehicles;
2. To the best of our knowledge, earlier works on controlling dynamic systems over the AWGN channel are mainly concerned with the stability and

state tracking of linear dynamic systems, e.g., [1,12,13,18,19,22,24,25,27,28]. Only the referenced studies [24,29] addressed the problem of controlling nonlinear dynamic systems over the AWGN channel. Nevertheless, this study [24] is just concerned with the estimation problem; and [29] addressed the problem of tracking and stability of those systems that have periodic outputs to sinusoidal inputs. Therefore, another study [29] used a linear dynamic system subject to saturated excitation for computer simulation as this type of noncommon dynamic systems was consistent with the theoretical development in [29]. However, by finding a describing function for the unicycle model, which also has periodic outputs to periodic inputs, this paper presents a real application of the theoretical development in [29] by controlling a practical nonlinear dynamic system over the AWGN channel.

1.3. Paper organization

The paper is organized as follows. In Section 2, the problem formulation is presented. Section 3 describes the describing function method. Then, Section 4 develops the theory of mean square reference tracking of linear dynamic systems with multiple real and non-real valued eigenvalues over MIMO AWGN channel. Section 5 is devoted to the tele-operation of autonomous vehicles. Section 6 gives simulation results for the unicycle model and Section 7 concludes this paper by summarizing the contributions of the paper and directions for future research.

2. Problem formulation

Throughout, certain conventions are used: $E[\cdot]$ denotes the expected value, $var[.]$ the variance, and $|\cdot|$ the absolute value and V' the transpose of vector/matrix V. A^{-1} denotes the inverse of a square matrix A and $N(m,n)$ is the Gaussian distribution with mean m and covariance n. $\mathbb{R}$ denotes the set of real numbers and I_n the identity matrix with dimension n by n. $trac(A)$, denotes the trace of a square matrix A, $diag\{.\}$ denotes the diagonal matrix, $[A]_{ij}$ denotes the i,jth element of the matrix A and $\underline{0}$ denotes the zero vector/matrix.

This paper is concerned with asymptotic mean square stability and reference tracking of autonomous vehicles over AWGN communication channel, as is shown in the block diagram of Figure 1. The building blocks of Figure 1 are described below.

Dynamic system: The dynamic system is the following time-invariant unicycle system [16]:

$$\begin{cases} \dot{x}(t) = v(t)\cos(\phi(t)) \\ \dot{y}(t) = v(t)\sin(\phi(t)) \\ \dot{\phi}(t) = u(t) \end{cases} \tag{1}$$

where $x(t)$ and $y(t)$ are the position vectors, $\phi(t)$ is the heading angle, and the control inputs are the vehicle forward velocity $v(t)$ and the angular velocity $u(t)$. Note that for the remote controller the initial conditions ($x(0)$, $y(0)$, $\phi(0)$) are unknown and have a Gaussian distribution.

Communication channel. Communication channel between system and controller is an MIMO AWGN channel without interference (parallel) with n inputs and n outputs. The output of the encoder (which will be described shortly) is transmitted through the MIMO channel and a white Gaussian noise vector is added to it (as is shown in Figure 1), where $N(t) = \begin{bmatrix} n_1(t) & . & . & . & n_n(t) \end{bmatrix}'$ i.i.d. $\sim N(\underline{0}, \tilde{R})$ ($\tilde{R} = diag\{\tilde{r}_1, ..., \tilde{r}_n\}$) is the MIMO channel noise and $n_i(t) \sim N(0, \tilde{r}_i)$ is the additive noise of the ith input - output path of the MIMO parallel AWGN channel. Also, the MIMO parallel AWGN channel is subject to the channel input power constraints Po_i, $i = 1, 2, ..., n$ as follows: $E[f_i^2(t)] \leq Po_i$, $i = 1, 2, ..., n$, where $f_i(t)$ is the ith element of the encoder output vector $F(t) = \begin{bmatrix} f_1(t) & . & . & . & f_n(t) \end{bmatrix}'$, which is the input of the channel. That is, $Y(t) = F(t) + N(t)$, where $Y(t) = \begin{bmatrix} y_1(t) & . & . & . & y_n(t) \end{bmatrix}'$ is the channel output.

Encoder. The encoder is a bandpass filter cascaded with a matrix gain. This bandpass filter saves only the fundamental frequency of the system outputs and omits the other harmonics which have less information to be sent. For this purpose, a high pass filter with a relatively low cut-off frequency (e.g., 0.1 Hz) is used to omit the DC part. This filter is cascaded with a low pass filter with a cut-off frequency of $\omega \gg 2\pi \times 0.1$ rad/s. For constructing such a filter, we can use the following transfer functions:

$$H_{bp}(s) = H_{hp}(s)H_{lp}(s), \tag{2}$$

$$H_{hp}(s) = \frac{s^2}{s^2 + \frac{\omega_h}{Q}s + \omega_h^2}, \quad \omega_h = 2\pi \times 0.1 \text{ rad/s},$$

$$Q = damping\ factor = 0.707, \tag{3}$$

$$H_{lp}(s) = \frac{\omega^2}{s^2 + \frac{\omega}{Q}s + \omega^2}. \tag{4}$$

It will be shown in the next section that the nonlinear dynamic system (1) together with the bandpass filter has an approximate linear dynamic system with $n = 7$ states $X(t) = \begin{bmatrix} x_1(t) & . & . & . & x_n(t) \end{bmatrix}'$, in which these states and the matrix gain

$$C(t) = \begin{bmatrix} c_{11}(t) & c_{12}(t) & ... & c_{1n}(t) \\ c_{21}(t) & c_{22}(t) & ... & c_{2n}(t) \\ & ... & & \\ c_{n1}(t) & c_{n2}(t) & ... & c_{nn}(t) \end{bmatrix},$$

form the encoder output as $F(t) = C(t)(X(t) - \hat{X}(t))$, where $\hat{X}(t) = \left[\hat{x}_1(t) \quad . \quad . \quad . \quad \hat{x}_n(t)\right]'$ is the estimation of states.

Decoder: Decoder is the minimum mean square estimator or the Kalman filter, also known as Linear Quadratic Estimator (LQE). At each time instant t, the Kalman filter generates an estimation $\hat{X}(t)$ using the channel output $Y(t)$.

Controller. Controller is a certainty equivalent controller of the following form: $u(t) = -l(t)\hat{X}(t) + \nu(t)$.

The objective of this paper is to find the matrix gain $C(t)$ and $u(t)$ to force the positions $x(t)$ and $y(t)$ and the heading angle $\phi(t)$ follows the desired paths.

3. Implementation of the describing function method

In this section, we first present the idea of the describing function to obtain the approximate linear dynamic system from a nonlinear time-invariant dynamic system. Then, we obtain the describing function for the nonlinear dynamic system of (1).

3.1. The Describing Function

This subsection is borrowed from [29]. For all nonlinear time - invariant dynamic systems that respond periodically to sinusoidal inputs, we can find an approximate linear dynamic system, as defined below [32].

Consider an Single-Input Single-Output (SISO) nonlinear time-invariant dynamic system with periodic outputs in response to periodic inputs. Suppose that this nonlinear dynamic system is excited by the following input: $u(t) = \gamma\cos(\omega t)$, where $\gamma > 0$ is large enough to excite all modes of the nonlinear system. Then, as the output is a periodic signal, it has a Fourier series representation that includes all harmonics of the input with frequency of ω. That is:

$$y(t) = y_d + \sum_{i=1}^{\infty}(a_i \sin(i\omega t) + b_i \cos(i\omega t)),$$

$$y_d = \frac{\omega}{4\pi}\int_{-\frac{2\pi}{\omega}}^{\frac{2\pi}{\omega}} y(t)dt,$$

$$a_i = \frac{\omega}{2\pi}\int_{-\frac{2\pi}{\omega}}^{\frac{2\pi}{\omega}} (y(t)\sin(i\omega t))dt,$$

$$b_i = \frac{\omega}{2\pi}\int_{-\frac{2\pi}{\omega}}^{\frac{2\pi}{\omega}} (y(t)\cos(i\omega t))dt. \tag{5}$$

Now, if this nonlinear system is cascaded with a bandpass filter with a high cut-off frequency of ω, then we have a periodic output at the end of the filter which consists of only the first harmonic with the frequency of ω, and all other harmonics are eliminated. In other words, the output of the bandpass filter is given in the following:

$$y_f(t) = a_1 \sin(\omega t) + b_1 \cos(\omega t). \tag{6}$$

Having that, we call the nonlinear dynamic system that is cascaded with the bandpass filter with the high cut-off frequency of ω, a quasi-linear system [32], because we can find a linear dynamic system with the input $u(t) = \gamma\cos(\omega t)$ and the output $y_f(t)$ with the following transfer function:

$$H(j\omega) = |H(j\omega)|\angle H(j\omega), \tag{7}$$

$$|H(j\omega)| = \frac{\sqrt{a_1^2 + b_1^2}}{\gamma}, \tag{8}$$

$$\angle H(j\omega) = -\arctan\left(\frac{a_1}{b_1}\right) \ rad. \tag{9}$$

This means that the nonlinear dynamic system can be represented by a linear dynamic system with the above transfer function called the describing function of the nonlinear dynamic system. Note that the describing function represents the transfer function of the approximate linear dynamic system and the transfer function represents the response of the dynamic system to the input signal when the initial conditions are set to be zero. Hence, the describing function is obtained for zero initial conditions.

3.2. The approximate linear system for the unicycle model

For a given fixed forward velocity $v(t)$, the nonlinear dynamic system (1) has periodic outputs to periodic inputs $u(t) = \gamma cos(\omega t)$. Hence, in the block diagram of Figure 1, as this dynamic is cascaded with the bandpass filter, it has an approximate linear system description. To obtain this describing function, we first assume that the input is $u(t) = \gamma\cos(\omega t)$; and $\dot{x}(t)$ and $\dot{y}(t)$ are the outputs of System (1), hence the inputs of the bandpass filter. Therefore, we obtain $H_{\dot{x}}(s) = \frac{f_1}{f_2 s^2 + f_3 s + f_4}$ and $H_{\dot{y}}(s) = \frac{c_1}{c_2 s^2 + c_3 2s + c_4}$ transfer functions as describing functions from the input to the outputs $\dot{x}(t)$ and $\dot{y}(t)$, respectively (f_is and c_is are real coefficients). Then, obviously for obtaining the describing functions from input $u(t)$ to outputs $x(t)$ and $y(t)$, we must multiply $\frac{1}{s}$ to these transfer functions. Note that as is clear from Figure 1, the inputs to the bandpass filter are $x(t)$ and $y(t)$. However, we can assume that these inputs are obtained by integration of $\dot{x}(t)$ and $\dot{y}(t)$; thus, for the simplicity of obtaining the describing functions, by moving this integration operator after the transfer function of the bandpass filter, we can assume that the outputs of the nonlinear system and the inputs to the filter are $\dot{x}(t)$ and $\dot{y}(t)$. Also, note that from Eq. (1), it follows that the transfer function

between input $u(t)$ and output $\phi(t)$ is $H_\phi(s) = \frac{1}{s}$. That is, the relation between $u(t)$ and $\phi(t)$ is linear.

The equivalent state space representation of the approximate linear system has seven states: $X(t) = [x_1(t)\ x_2(t),\ \ldots,x_7(t)]'$ which correspond to $d_1\ddot{x}(t) + d_2\dot{x}(t) + x(t)$, $d_3\ddot{x}(t) + d_4\dot{x}(t)$, $d_5\ddot{x}(t) + d_6\dot{x}(t)$, $d_7\ddot{y}(t) + d_8\dot{y}(t) + y(t)$, $d_9\ddot{y}(t) + d_{10}\dot{y}(t)$, $d_{11}\ddot{y}(t) + d_{12}\dot{y}(t)$ and $\phi(t)$, respectively (d_is are real coefficients). The input of this representation is $u(t)$ and the output vector is $[x(t)\ y(t)\ \phi(t)]'$ with the system matrices:

$$A = \begin{bmatrix} A_x & \underline{0} & \underline{0} \\ \underline{0} & A_y & \underline{0} \\ \underline{0} & \underline{0} & A_\phi \end{bmatrix}, \qquad B = [B_x \ \ B_y \ \ B_\phi]'$$

$$C = \begin{bmatrix} C_x & \underline{0} & \underline{0} \\ \underline{0} & C_y & \underline{0} \\ \underline{0} & \underline{0} & C_\phi \end{bmatrix},$$

where:

$$A_x = \begin{bmatrix} 0 & 0 & 0 \\ 0 & e_1 & e_2 \\ 0 & -e_2 & e_1 \end{bmatrix}, \quad A_y = \begin{bmatrix} 0 & 0 & 0 \\ 0 & e_5 & e_6 \\ 0 & -e_6 & e_5 \end{bmatrix},$$

$$A_\phi = 0, \quad B_x = [e_9\ e_{10}\ e_{11}], \quad B_y = [e_{12}\ e_{13}\ e_{14}],$$

$$B_\phi = 1, C_x = [e_{15}\ e_{16}\ 0], \qquad C_y = [e_{17}\ e_{18}\ 0],$$

$$C_\phi = 1.$$

Hence, we need a MIMO parallel AWGN channel with 7 inputs and 7 outputs for transmitting $x_1(t)$ to $x_7(t)$. Note that the equivalent state space representation of the approximate linear system is in the real Jordan form.

4. Reference tracking of linear systems with multiple real and non-real valued eigenvalues over AWGN channel

Now, we extend the results of [13] to account for reference tracking and hence, the stability of linear dynamic systems with multiple real and non-real valued eigenvalues over MIMO parallel AWGN channel. In the next section, by applying these extended results on the describing functions associated with the nonlinear system (1), we address the reference tracking problem of tele-operation of autonomous vehicles, as is shown in the block diagram of Figure 1.

Suppose that the dynamic system in Figure 1 is linear with n states. Hence, the system that is seen by the remote controller is as follows:

$$\begin{cases} \dot{X}(t) = AX(t) + Bu(t),\ X(0) = \xi, \\ Y(t) = C(t)(X(t) - \hat{X}(t)) + N(t) \end{cases} \tag{10}$$

where $X(0)$ is the initial state that is known for the encoder, but is unknown for the remote controller, that is, for the remote controller the exact value of ξ is unknown and hence $\xi \sim N(X_0, Q_0)$ (Q_0 is diagonal) is treated as the Gaussian random variable with known mean and variance. Note that $N(t) = \begin{bmatrix} n_1(t) & . & . & . & n_n(t) \end{bmatrix}'$ $i.i.d. \sim N(\underline{0}, \tilde{R})$ ($\tilde{R} = diag\{\tilde{r}_1, ..., \tilde{r}_n\}$) is the additive noise of the MIMO channel and ($n_i(t) \sim N(0, \tilde{r}_i)$ is the additive noise of the ith path of the MIMO parallel AWGN channel, which can be treated as the measurement noise provided the channel input power constraint is met. The objective here is to achieve mean square asymptotic reference tracking for the linear system (10) with n states and n outputs over the MIMO parallel AWGN channel.

Throughout, it is assumed that the system matrix A has real eigenvalues real multiple eigenvalues and distinct complex conjugate eigenvalues as the system matrix A that corresponds to the describing function of the nonlinear system (1) including these types of eigenvalues. According to the previous section, for the unicycle model, the system matrix A of the approximate linear system is in the real Jordan form. Therefore, throughout this section, it is assumed that System (10) can be decomposed to several decoupled sub-systems; hence, for each sub-system, an encoder and a decoder are designed separately. Note that the Jordan block associated with a real eigenvalue $\lambda_i(A)$ with multiplicity 2 is the following matrix:

$$\begin{bmatrix} \lambda_i(A) & 1 \\ 0 & \lambda_i(A) \end{bmatrix},$$

and the Jordan block associated with the complex conjugate pair of eigenvalues $\lambda_i(A) = \sigma \pm \sqrt{-1}w$ ($w \neq 0$) is $\begin{bmatrix} \sigma & w \\ -w & \sigma \end{bmatrix}$.

4.1. Mean square asymptotic state tracking

In this section, it is assumed that each of the Jordan block is at most a 2 by 2 matrix. Then, for all three possible cases:

a) $A = \begin{bmatrix} \sigma & w \\ -w & \sigma \end{bmatrix}$, $\sigma, w \in \mathbb{R}, w \neq 0$,

b) $A = \begin{bmatrix} a & 1 \\ 0 & a \end{bmatrix}$, $a \in \mathbb{R}$,

c) $A = \begin{bmatrix} a_1 & 0 \\ 0 & a_2 \end{bmatrix}$, $a_1, a_2 \in \mathbb{R}, a_1 \neq a_2$,

we find the matrix gain $C(t)$ for mean square asymptotic state tracking of system states at the decoder.

4.1.1. Sub-systems with complex conjugate eigenvalues

Suppose that the system matrix A in the linear system of (10) has the following form:

$$A = \begin{bmatrix} \sigma & w \\ -w & \sigma \end{bmatrix}, \quad \sigma, w \in \mathbb{R}, \quad w \neq 0. \tag{11}$$

Then, we have the following proposition for mean square asymptotic state tracking of system states at the decoder.

Proposition 4.1. Consider the block diagram of Figure 1 described by the linear system (10) with the system matrix $A = \begin{bmatrix} \sigma & w \\ -w & \sigma \end{bmatrix}, \sigma, w \in \mathbb{R}, w \neq 0$. Suppose that $Po_1 > 2\sigma$ and $Po_2 > 2\sigma$, $[Q_0]_{12} = 0$, $[Q_0]_{11} = [Q_0]_{22}$ and $\tilde{r}_1 = \tilde{r}_2$. Let $\gamma_1 = \min(Po_1, Po_2)$. Then, by choosing the encoder matrix gain as:

$$C(t) = \begin{bmatrix} \sqrt{\frac{\gamma_1 \tilde{r}_1}{p_{11}(t)}} & 0 \\ 0 & \sqrt{\frac{\gamma_1 \tilde{r}_2}{p_{22}(t)}} \end{bmatrix},$$

and the following decoder:

$$\dot{\hat{X}}(t) = A\hat{X}(t) + Bu(t) + K(t)Y(t), \quad \hat{X}(0) = X_0, \quad (12)$$

$$K(t) = P(t)C'(t)\tilde{R}^{-1}, \quad \tilde{R} = diag\{\tilde{r}_1, \tilde{r}_2\}, \quad (13)$$

$$\dot{P}(t) = A'P(t) + P(t)A - P(t)C'(t)\tilde{R}^{-1}C(t)P(t),$$

$$P(0) = Q_0, \quad P(t) = P'(t) = \begin{bmatrix} p_{11}(t) & p_{12}(t) \\ p_{12}(t) & p_{22}(t) \end{bmatrix} \geq 0, \quad (14)$$

we have mean square asymptotic state tracking of system states at the decoder.

Proof. The encoder matrix gain has the following general form:

$$C(t) = \begin{bmatrix} c_{11}(t) & c_{12}(t) \\ c_{21}(t) & c_{22}(t) \end{bmatrix},$$

subsequently, the decoder can be extracted by Eq. (15) as shown in Box I (for the simplicity of presentation, the dependency on the time index, t, is dropped). Now, by substituting $c_{11}(t) = \sqrt{\frac{\gamma_1 \tilde{r}_1}{p_{11}(t)}}$, $c_{22}(t) = \sqrt{\frac{\gamma_1 \tilde{r}_2}{p_{22}(t)}}$ and $c_{12}(t) = c_{21}(t) = 0$, we have $\dot{p}_{12}(t) = 0$ ($\Rightarrow p_{12}(t) = p_{12}(0) = [Q_0]_{12} = 0$) and:

$$\dot{p}_{11}(t) = (2\sigma - \gamma_1)p_{11}(t) \Rightarrow p_{11}(t) = e^{-(\gamma_1 - 2\sigma)t}p_{11}(0). \quad (16)$$

$$\dot{p}_{22}(t) = (2\sigma - \gamma_1)p_{22}(t) \Rightarrow p_{22}(t) = e^{-(\gamma_1 - 2\sigma)t}p_{22}(0). \quad (17)$$

Thus, in the above selection, we have:

$$P(t) = \begin{bmatrix} e^{-(\gamma_1 - 2\sigma)t}p_{11}(0) & 0 \\ 0 & e^{-(\gamma_1 - 2\sigma)t}p_{22}(0) \end{bmatrix}, \quad (18)$$

when the decoder description is as follows:

$$\dot{\hat{X}}(t) = A\hat{X}(t) + Bu(t) + K(t)Y(t), \quad \hat{X}(0) = X_0,$$

$$K(t) = P(t)C'(t)\tilde{R}^{-1}. \quad (19)$$

Now, assuming that $\gamma_1 > 2\sigma$, we have:

$$\lim_{t\to\infty} E[(x_1(t) - \hat{x}_1(t))^2] = \lim_{t\to\infty} p_{11}(t)$$

$$= \lim_{t\to\infty} e^{-(\gamma_1 - 2\sigma)t}p_{11}(0) = 0.$$

Similarly, we have:

$$\lim_{t\to\infty} E[(x_2(t) - \hat{x}_2(t))^2] = \lim_{t\to\infty} p_{22}(t) = 0.$$

Hence:

$$P(t) \to \bar{P} = \begin{bmatrix} 0 & 0 \\ 0 & 0 \end{bmatrix}.$$

This completes the proof.

4.1.2. Sub-systems with real multiple eigenvalues
Suppose that the system matrix A in the linear system of (10) has the following form:

$$A = \begin{bmatrix} a & 1 \\ 0 & a \end{bmatrix}, a \in \mathbb{R}. \quad (20)$$

Then, we have the following proposition for mean square asymptotic state tracking of system states at the decoder:

$$\begin{aligned}
\dot{p}_{11} &= 2\sigma p_{11} - 2wp_{12} - (2p_{11}p_{12}c_{11}c_{12}\tilde{r}_1^{-1} + 2p_{11}p_{12}c_{21}c_{22}\tilde{r}_2^{-1} + p_{11}^2c_{11}^2\tilde{r}_1^{-1} + p_{12}^2c_{12}^2\tilde{r}_1^{-1} \\
&\quad + p_{11}^2c_{21}^2\tilde{r}_2^{-1} + p_{12}^2c_{22}^2\tilde{r}_2^{-1}) \\
\dot{p_{22}} &= 2\sigma p_{22} + 2wp_{12} - (2p_{22}p_{12}c_{22}c_{21}\tilde{r}_2^{-1} + 2p_{22}p_{12}c_{21}c_{11}\tilde{r}_1^{-1} + p_{22}^2c_{22}^2\tilde{r}_2^{-1} + p_{12}^2c_{21}^2\tilde{r}_2^{-1} \\
&\quad + p_{22}^2c_{12}^2\tilde{r}_1^{-1} + p_{12}^2c_{11}^2\tilde{r}_1^{-1}) \\
\dot{p_{12}} &= 2\sigma p_{12} - wp_{22} + wp_{11} - \tilde{r}_1^{-1}(p_{11}p_{12}c_{11}^2 + p_{12}^2c_{11}c_{12} + p_{11}p_{22}c_{11}c_{12} + p_{12}p_{22}c_{12}^2) \\
&\quad - \tilde{r}_2^{-1}(p_{11}p_{12}c_{21}^2 + p_{12}^2c_{22}c_{21} + p_{11}p_{22}c_{22}c_{21} + p_{12}p_{22}c_{22}^2)
\end{aligned} \quad (15)$$

Box I

Proposition 4.2. Consider the block diagram of Figure 1 described by the linear system (10) with the system matrix $A = \begin{bmatrix} a & 1 \\ 0 & a \end{bmatrix}$, $a \in \mathbb{R}$. Suppose that $Po_1 > 2a$ and $Po_2 > 2a$, $[Q_0]_{12} = 0$, $[Q_0]_{11} = [Q_0]_{22}$, and $\tilde{r}_1 = \tilde{r}_2$. Then, by choosing the encoder matrix gain as:

$$C(t) = \begin{bmatrix} \sqrt{\frac{\tilde{r}_1}{2\delta p_{11}(t)}} & \sqrt{\frac{\delta \tilde{r}_1}{2p_{22}(t)}} \\ \sqrt{\frac{\delta \tilde{r}_2}{2p_{11}(t)}} & \sqrt{\frac{\tilde{r}_2}{2\delta p_{22}(t)}} \end{bmatrix},$$

where $\delta = \gamma_1 - \sqrt{\gamma_1^2 - 1}$ and $\gamma_1 = \min(Po_1, Po_2)$, and the following decoder:

$$\dot{\hat{X}}(t) = A\hat{X}(t) + Bu(t) + K(t)Y(t), \quad \hat{X}(0) = X_0, \quad (21)$$

$$K(t) = P(t)C'(t)\tilde{R}^{-1}, \quad \tilde{R} = diag\{\tilde{r}_1, \tilde{r}_2\}, \quad (22)$$

$$\dot{P}(t) = A'P(t) + P(t)A - P(t)C'(t)\tilde{R}^{-1}C(t)P(t),$$

$$P(0) = Q_0, P(t) = P'(t) = \begin{bmatrix} p_{11}(t) & p_{12}(t) \\ p_{12}(t) & p_{22}(t) \end{bmatrix} \geq 0, \quad (23)$$

we have mean square asymptotic state tracking of system states at the decoder.

Proof. The encoder matrix gain has the following general form:

$$C(t) = \begin{bmatrix} c_{11}(t) & c_{12}(t) \\ c_{21}(t) & c_{22}(t) \end{bmatrix},$$

subsequently, the decoder can be extracted by Eq. (24) as shown in Box II (for the simplicity of presentation, the dependency on the time index, t, is omitted). Now, by substituting:

$$c_{11}(t) = \sqrt{\frac{\tilde{r}_1}{2\delta p_{11}(t)}}, \qquad c_{12}(t) = \sqrt{\frac{\delta \tilde{r}_1}{2p_{22}(t)}},$$

$$c_{21}(t) = \sqrt{\frac{\delta \tilde{r}_2}{2p_{11}(t)}}, \qquad c_{22}(t) = \sqrt{\frac{\tilde{r}_2}{2\delta p_{22}(t)}},$$

we have $\dot{p}_{12}(t) = 0$ ($\Rightarrow p_{12}(t) = p_{12}(0) = [Q_0]_{12} = 0$) and:

$$\dot{p}_{11}(t) = \left(2a - \left(\frac{1}{2\delta} + \frac{\delta}{2}\right)\right) p_{11}(t) \Rightarrow \dot{p}_{11}(t)$$

$$= \left(2a - \frac{1+\delta^2}{2\delta}\right) p_{11}(t) \Rightarrow, \quad (25)$$

$$\dot{p}_{11}(t) = (2a - \gamma_1)p_{11}(t) \Rightarrow p_{11}(t) = e^{-(\gamma_1 - 2a)t}p_{11}(0), \quad (26)$$

$$\dot{p}_{22}(t) = \left(2a - \left(\frac{1}{2\delta} + \frac{\delta}{2}\right)\right) p_{22}(t) \Rightarrow \dot{p}_{22}(t)$$

$$= \left(2a - \frac{1+\delta^2}{2\delta}\right) p_{22}(t) \Rightarrow, \quad (27)$$

$$\dot{p}_{22}(t) = (2a - \gamma_1)p_{22}(t) \Rightarrow p_{22}(t) = e^{-(\gamma_1 - 2a)t}p_{22}(0). \quad (28)$$

Thus, by the above selection, we have:

$$P(t) = \begin{bmatrix} e^{-(\gamma_1 - 2a)t}p_{11}(0) & 0 \\ 0 & e^{-(\gamma_1 - 2a)t}p_{22}(0) \end{bmatrix}, \quad (29)$$

when the decoder description is as follows:

$$\dot{\hat{X}}(t) = A\hat{X}(t) + Bu(t) + K(t)Y(t), \quad \hat{X}(0) = X_0,$$

$$K(t) = P(t)C'(t)\tilde{R}^{-1}. \quad (30)$$

$$\begin{aligned}
\dot{p}_{11} &= 2ap_{11} - (2p_{11}p_{12}c_{11}c_{12}\tilde{r}_1^{-1} + 2p_{11}p_{12}c_{21}c_{22}\tilde{r}_2^{-1} + p_{11}^2c_{11}^2\tilde{r}_1^{-1} + p_{12}^2c_{12}^2\tilde{r}_1^{-1} \\
&\quad + p_{11}^2c_{21}^2\tilde{r}_2^{-1} + p_{12}^2c_{22}^2\tilde{r}_2^{-1}) \\
\dot{p_{22}} &= 2ap_{22} + 2p_{12} - (2p_{22}p_{12}c_{22}c_{21}\tilde{r}_2^{-1} + 2p_{22}p_{12}c_{21}c_{11}\tilde{r}_1^{-1} + p_{22}^2c_{22}^2\tilde{r}_2^{-1} + p_{12}^2c_{21}^2\tilde{r}_2^{-1} \\
&\quad + p_{22}^2c_{12}^2\tilde{r}_1^{-1} + p_{12}^2c_{11}^2\tilde{r}_1^{-1}) \\
\dot{p_{12}} &= 2ap_{12} + p_{11} - \tilde{r}_1^{-1}(p_{11}p_{12}c_{11}^2 + p_{12}^2c_{11}c_{12} + p_{11}p_{22}c_{11}c_{12} + p_{12}p_{22}c_{12}^2) \\
&\quad - \tilde{r}_2^{-1}(p_{11}p_{12}c_{21}^2 + p_{12}^2c_{22}c_{21} + p_{11}p_{22}c_{22}c_{21} + p_{12}p_{22}c_{22}^2)
\end{aligned} \quad (24)$$

Box II

Now, assuming that $Po_1 > 2a$ and $Po_2 > 2a$, we have $\lim_{t\to\infty} E[(x_1(t) - \hat{x}_1(t))^2] = \lim_{t\to\infty} p_{11}(t) = \lim_{t\to\infty} e^{-(\gamma_1-2a)t}p_{11}(0) = 0$. Similarly, we have $\lim_{t\to\infty} E[(x_2(t) - \hat{x}_2(t))^2] = \lim_{t\to\infty} p_{22}(t) = 0$. Hence, $P(t) \to \bar{P} = \begin{bmatrix} 0 & 0 \\ 0 & 0 \end{bmatrix}$. This completes the proof.

4.1.3. Sub-systems with real distinct eigenvalues

Suppose that the system matrix A in the linear system of (10) has the following form:

$$A = \begin{bmatrix} a_1 & 0 \\ 0 & a_2 \end{bmatrix}, \quad a_1, a_2 \in \mathbb{R},\ a_1 \neq a_2. \tag{31}$$

Then, we have the following proposition for mean square asymptotic state tracking of system states at the decoder:

Proposition 4.3. Consider the block diagram of Figure 1 described by the linear system (10) with the system matrix $A = \begin{bmatrix} a_1 & 0 \\ 0 & a_2 \end{bmatrix}$, $a_1, a_2 \in \mathbb{R}, a_1 \neq a_2$. Suppose that $[Q_0]_{12} = 0$, $Po_1 > 2a_1$ and $Po_2 > 2a_2$ (Po_1 and Po_2 are the channel input power constraint). Then, by choosing the encoder matrix gain as:

$$C(t) = \begin{bmatrix} \sqrt{\frac{Po_1\tilde{r}_1}{p_{11}(t)}} & 0 \\ 0 & \sqrt{\frac{Po_2\tilde{r}_2}{p_{22}(t)}} \end{bmatrix},$$

and a decoder with the following description:

$$\dot{\hat{X}}(t) = A\hat{X}(t) + Bu(t) + K(t)Y(t),$$

$$\hat{X}(0) = X_0, \tag{32}$$

$$K(t) = P(t)C'(t)\tilde{R}^{-1}, \quad \tilde{R} = diag\{\tilde{r}_1, \tilde{r}_2\}, \tag{33}$$

$$\dot{P}(t) = A'P(t) + P(t)A - P(t)C'(t)\tilde{R}^{-1}C(t)P(t),$$

$$P(0) = Q_0, P(t) = P'(t) = \begin{bmatrix} p_{11}(t) & p_{12}(t) \\ p_{12}(t) & p_{22}(t) \end{bmatrix} \geq 0, \tag{34}$$

we have mean square asymptotic state tracking of system states at the decoder.

Proof. The encoder matrix gain has the following general form:

$$C(t) = \begin{bmatrix} c_{11}(t) & c_{12}(t) \\ c_{21}(t) & c_{22}(t) \end{bmatrix},$$

subsequently, the matrix $P(t)$ which represents the covariance matrix of the decoding error can be extracted by Eq. (35) as shown in Box III (for the simplicity of presentation, the dependency on the time index t is dropped). Now, by substituting $c_{11}(t) = \sqrt{\frac{Po_1\tilde{r}_1}{p_{11}(t)}}$, $c_{22}(t) = \sqrt{\frac{Po_2\tilde{r}_2}{p_{22}(t)}}$ and $c_{12}(t) = c_{21}(t) = 0$, we have $\dot{p}_{12}(t) = 0$ and $p_{12}(t) = p_{12}(0) = [Q_0]_{12} = 0$. Subsequently, we have:

$$\dot{p}_{11}(t) = (2a_1 - Po_1)p_{11}(t) \Rightarrow p_{11}(t) = e^{-(Po_1-2a_1)t}p_{11}(0), \tag{36}$$

$$\dot{p}_{22}(t) = (2a_2 - Po_2)p_{22}(t) \Rightarrow p_{22}(t) = e^{-(Po_2-2a_2)t}p_{22}(0). \tag{37}$$

Thus, by the above selection, we have:

$$P(t) = \begin{bmatrix} e^{-(Po_1-2a_1)t}p_{11}(0) & 0 \\ 0 & e^{-(Po_2-2a_2)t}p_{22}(0) \end{bmatrix}, \tag{38}$$

when the decoder description is as follows:

$$\dot{\hat{X}}(t) = A\hat{X}(t) + Bu(t) + K(t)Y(t), \quad \hat{X}(0) = X_0,$$

$$K(t) = P(t)C'(t)\tilde{R}^{-1}. \tag{39}$$

Now, assuming that $Po_1 > 2a_1$ and $Po_2 > 2a_2$, we have:

$$\lim_{t\to\infty} E[(x_1(t) - \hat{x}_1(t))^2] = \lim_{t\to\infty} p_{11}(t) = \lim_{t\to\infty} e^{-(Po_1-2a_1)t}p_{11}(0) = 0.$$

$$\begin{aligned}
\dot{p_{11}} &= 2a_1p_{11} - (2p_{11}p_{12}c_{11}c_{12}\tilde{r}_1^{-1} + 2p_{11}p_{12}c_{21}c_{22}\tilde{r}_2^{-1} + p_{11}^2c_{11}^2\tilde{r}_1^{-1} + p_{12}^2c_{12}^2\tilde{r}_1^{-1} \\
&\quad + p_{11}^2c_{21}^2\tilde{r}_2^{-1} + p_{12}^2c_{22}^2\tilde{r}_2^{-1}) \\
\dot{p_{22}} &= 2a_2p_{22} - (2p_{22}p_{12}c_{22}c_{21}\tilde{r}_2^{-1} + 2p_{22}p_{12}c_{21}c_{11}\tilde{r}_1^{-1} + p_{22}^2c_{22}^2\tilde{r}_2^{-1} + p_{12}^2c_{21}^2\tilde{r}_2^{-1} \\
&\quad + p_{22}^2c_{12}^2\tilde{r}_1^{-1} + p_{12}^2c_{11}^2\tilde{r}_1^{-1}) \\
\dot{p_{12}} &= a_1p_{12} + a_2p_{12} - \tilde{r}_1^{-1}(p_{11}p_{12}c_{11}^2 + p_{12}^2c_{11}c_{12} + p_{11}p_{22}c_{11}c_{12} + p_{12}p_{22}c_{12}^2) \\
&\quad - \tilde{r}_2^{-1}(p_{11}p_{12}c_{21}^2 + p_{12}^2c_{22}c_{21} + p_{11}p_{22}c_{22}c_{21} + p_{12}p_{22}c_{22}^2)
\end{aligned} \tag{35}$$

Box III

Similarly, we have:

$$\lim_{t\to\infty} E[(x_2(t)-\hat{x}_2(t))^2] = \lim_{t\to\infty} p_{22}(t) = 0.$$

Hence:

$$P(t) \to \bar{P} = \begin{bmatrix} 0 & 0 \\ 0 & 0 \end{bmatrix}.$$

This completes the proof.

4.2. Asymptotic reference tracking

Now, to obtain the control signal $u(t)$ for tracking the reference signal $R(t)$, we consider the following cost functional:

$$J = \lim_{t_1\to\infty} \frac{1}{t_1} \int_0^{t_1} E[[X(t)-R(t)]'Q[X(t)-R(t)] + ru^2(t)]dt, \quad Q = Q' \geq 0, \quad r > 0. \tag{40}$$

Subsequently, the control signal $u(t)$ is obtained by minimizing the above cost functional subject to the dynamic system (10). From the classical LQG results [33], it follows that $u(t) = -l(t)\hat{X}(t) + \nu(t)$, where:

$$l(t) = r^{-1}B'\tilde{P}(t), \tag{41}$$

$$\nu(t) = -r^{-1}B'S(t), \tag{42}$$

and $\tilde{P}(t)$ and $S(t)$ are the solutions of the following equations:

$$\dot{\tilde{P}}(t) = -\tilde{P}(t)A - A'\tilde{P}(t) - Q + \tilde{P}(t)Br^{-1}B'\tilde{P}(t), \tag{43}$$

$$\dot{S}(t) = -[A' - \tilde{P}(t)Br^{-1}B']S(t) + QR(t). \tag{44}$$

Under the assumption that the pair (A, B) is stabilizable and the pair (I_n, A) is detectable, we have $\tilde{P}(t) \to \bar{\tilde{P}}$ [33], where $\bar{\tilde{P}}$ is the unique symmetric non-negative definite stabilizing solution of the corresponding Algebraic Riccati equation; hence, $J \to \bar{J} = 0$. This indicates that $E[X(t)-R(t)]'Q[X(t)-R(t)] \to 0$; and hence, $E[(x_i(t)-r_i(t))^2] \to 0$, $i = 1, 2, ..., n$, $(R(t) = \begin{bmatrix} r_1(t) & . & . & . & r_n(t) \end{bmatrix}')$.

5. Reference tracking of the tele-operation of autonomous vehicles

In this section, the results of previous sections are applied to address the reference tracking problem of the tele-operation system described by the block diagram of Figure 1. In this block diagram, the nonlinear dynamics of the miniature drones, autonomous road vehicles, and autonomous underwater vehicles are described by the unicycle model of (1). In this tele-operation system, the initial conditions vector $\begin{bmatrix} x(0) & y(0) & \phi(0) \end{bmatrix}'$ is unknown for the remote controller and has the Gaussian distribution with diagonal covariance matrix. Both positions $x(t)$ and $y(t)$ must be controlled by one input $u(t)$ as it is assumed that the forward velocity $v(t)$ is fixed. In the following, $r_\phi(t)$, $r_x(t)$, and $r_y(t)$ are the reference signals for $\phi(t)$, $x(t)$, and $y(t)$, respectively $(R(t) = [r_x(t)\ r_y(t)\ r_\phi(t)]')$, and $\hat{x}(t)$, $\hat{y}(t)$ and $\hat{\phi}(t)$ are mean square estimation of $x(t)$, $y(t)$, and $\phi(t)$ at the decoder, respectively, which are available for the remote controller. Now, from Figure 2 it follows that to control both $x(t)$ and $y(t)$ by one input $u(t)$, we must have the reference signal $r_\phi(t) = \arctan(\frac{r_y(t)-\hat{y}(t)}{r_x(t)-\hat{x}(t)})$ [34], which forces $x(t)$ and $y(t)$ to follow $r_x(t)$ and $r_y(t)$, respectively, when $\phi(t)$ tracks $r_\phi(t)$ and $\hat{x}(t) \to x(t)$, $\hat{y}(t) \to y(t)$.

To this end, we notice that the equivalent state space representation of the approximate linear system of the nonlinear unicycle model cascaded with the bandpass filter, has seven states: $X(t) = [x_1(t)\ x_2(t)\ .\ .\ .\ x_7(t)]'$; hence, we need an MIMO parallel AWGN channel with 7 inputs and 7 outputs for transmitting $x_1(t)$ to $x_7(t)$. Now, we use the encoder and decoder proposed in the previous section with matrices derived from A, B, and C, as given in Section 3. Since the system matrix A is in the real Jordan form, the encoder and decoder proposed in Section 4 can be used for different 2 by 2 sub-systems for transmitting $[x_2(t)\ x_3(t)]'$ and $[x_5(t)\ x_6(t)]'$ and their reconstruction at the decoder, and, also, for the scalar sub-systems for transmitting $x_1(t)$, $x_4(t)$, and $x_7(t)$ and their reconstruction. Then, using the controller $u(t) = -l(t)\hat{\phi}(t) + \nu(t)$ with gains computed by Eqs. (41) to (44) with $A = A_\phi = 0$, $B = B_\phi = 1$, and $R(t) = r_\phi(t)$, we have mean square asymptotic

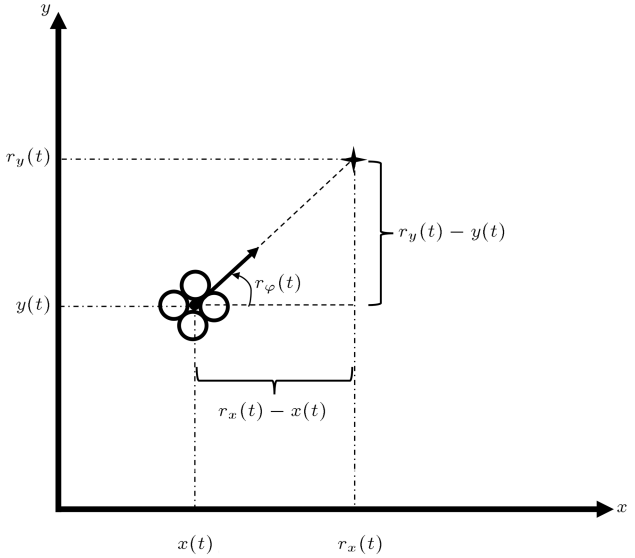

Figure 2. An autonomous vehicle with current positions $x(t)$ and $y(t)$ moving towards the desired positions $r_x(t)$ and $r_y(t)$.

tracking of the reference signal $r_\phi(t)$ by $\phi(t)$, and, hence, the desired reference tracking. Note that at the decoder, $\hat{x}(t)$, $\hat{y}(t)$, and $\hat{\phi}(t)$ are obtained as follows: $[\hat{x}(t)\ \hat{y}(t)\ \hat{\phi}(t)]' = C\hat{X}(t)$, which converge to $[x(t)\ y(t)\ \phi(t)]' = CX(t)$, as $\hat{X}(t) \to X(t)$ in mean square sense.

6. Simulation results

For the purpose of illustration, consider the block diagram of Figure 1 with the nonlinear dynamic of (1). For the remote controller, the initial conditions $(x(0), y(0), \phi(0))$ are unknown and have the following description $[x(t)\ y(t)\ \phi(t)]' \sim N(\underline{0}, 3I_3)$. The autonomous vehicle must track a circle with the center located at (x_r, y_r) and the radius of ρ with the angular velocity of ω_r. Therefore, $[x(t)\ y(t)\ \phi(t)]'$ must track the reference signal $[r_x(t)\ r_y(t)\ r_\phi(t)]'$, where $r_x(t) = x_r + \rho\cos(\omega_r t)$, $r_y(t) = y_r + \rho\sin(\omega_r t)$ and $r_\phi(t) = \arctan(\frac{r_y(t)-\hat{y}(t)}{r_x(t)-\hat{x}(t)})$. Note that as $\dot{r}_x(t) = \rho\omega_r\sin(-\omega_r t)$ and $\dot{r}_y(t) = \rho\omega_r\cos(-\omega_r t)$, for the simplicity of design, we choose the forward velocity constant and equal to $v(t) = \rho\omega_r$ m/s.

To obtain the describing function for a given ω, e.g., $\omega = 1$ rad/s, we apply the inputs $v(t) = \rho\omega_r$ m/s and $u(t) = \eta\omega_r\cos(\omega t)$ rad/s ($\eta \geq 1$ is a gain to excite all modes of the nonlinear system) to System (1). Then, from this input and the corresponding outputs of the bandpass filter, the describing functions for $\eta = 3$, $\omega_r = 1$ rad/s and $\rho = 1$ are computed as $H_x(s) = \frac{1}{s(s^2+0.2s+8.5)}$ and $H_y(s) = \frac{-1}{s(s^2+0.2s+8.5)}$, respectively. The equivalent linear state space representation of this system has seven states: $X(t) = [x_1(t),\ x_2(t),\ \ldots,\ x_7(t)]'$ which correspond to $0.1176\ddot{x}(t)+0.0235\dot{x}(t)+x(t)$, $-0.1176\ddot{x}(t)-0.0235\dot{x}(t)$, $0.0040\ddot{x}(t)-0.3424\dot{x}(t)$, $0.1176\ddot{y}(t)+0.0235\dot{y}(t)+y(t)$, $-0.1176\ddot{y}(t)-0.0235\dot{y}(t)$, $0.0040\ddot{y}(t)-0.3424\dot{y}(t)$ and $\phi(t)$, respectively. The input of this representation is $u(t)$ and the output vector is $[x(t)\ y(t)\ \phi(t)]'$ with the system matrices:

$$A = \begin{bmatrix} A_x & \underline{0} & \underline{0} \\ \underline{0} & A_y & \underline{0} \\ \underline{0} & \underline{0} & A_\phi \end{bmatrix}, \qquad B = [B_x\ \ B_y\ \ B_\phi]',$$

$$C = \begin{bmatrix} C_x & \underline{0} & \underline{0} \\ \underline{0} & C_y & \underline{0} \\ \underline{0} & \underline{0} & C_\phi \end{bmatrix},$$

where:

$$A_x = \begin{bmatrix} 0 & 0 & 0 \\ 0 & -0.1 & -2.914 \\ 0 & 2.914 & -0.1 \end{bmatrix},$$

$$A_y = \begin{bmatrix} 0 & 0 & 0 \\ 0 & -0.1 & -2.914 \\ 0 & 2.914 & -0.1 \end{bmatrix}, \qquad A_\phi = 0,$$

$$B_x = [0.1176\ \ -0.1176\ 0.0040],$$

$$B_y = [0.1176\ \ -0.1176\ 0.0040], \qquad B_\phi = 1,$$

$$C_x = [1\ 1\ 0], \quad C_y = [-1\ \ -1\ 0], \qquad C_\phi = 1.$$

Hence, we need a MIMO parallel AWGN channel with 7 inputs and 7 outputs for transmitting $x_1(t)$ to $x_7(t)$, which has the following specification:

$$N(t)\ i.i.d. \sim N(\underline{0}, diag\{0.5, 0.5, 0.5, 0.5, 0.5, 0.5, 0.5\})$$

with the power constraints: $Po_i = 1$ for $i \in \{1, 2, 3, ..., 7\}$, which meet the requirements of the propositions of Section 4.

Figure 3 to Figure 5 illustrate that the system outputs $x(t)$, $y(t)$, and $\phi(t)$ track the reference signals $r_x(t)$, $r_y(t)$, and $r_\phi(t)$, respectively, for $\eta = 3$, $\rho = 1$, $\omega_r = 1$, and $x_r = y_r = 0$ using the technique proposed in Section 5. Figure 6 illustrates the control signal $u(t)$. Also, Figures 7 and 8 illustrate that the autonomous vehicle tracks the reference circle. As is clear from these figures, the proposed tracking technique is able to force the nonlinear system asymptotically to track the reference signals very well. The Root Cumulative Square Error (RCSE) computed for the period of [20, 50] second (i.e., $\sqrt{\int_{20}^{50}[(x(t)-r_x(t))^2+(y(t)-r_y(t))^2]dt}$) for different choices of ω is shown in Table 1.

This table indicates that in order to have a satisfactory reference tracking, the high cut off frequency of the bandpass filter is better to be at least equal to ω_r.

To compare the performance of the proposed technique, we apply the proposed technique and the

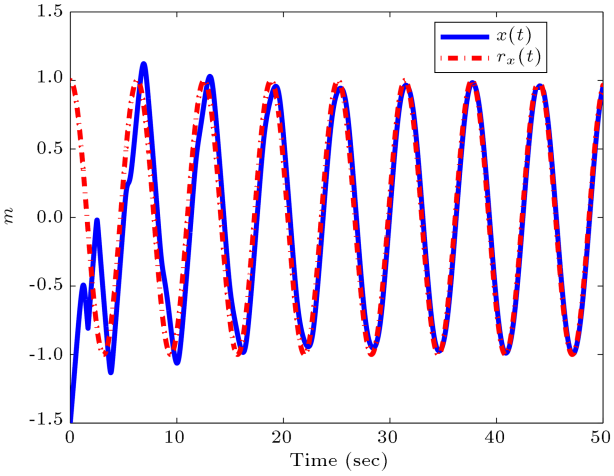

Figure 3. $x(t)$ position of the system and its reference signal $r_x(t)$. It is observed that after less than 4 seconds $x(t)$ converges to $r_x(t)$.

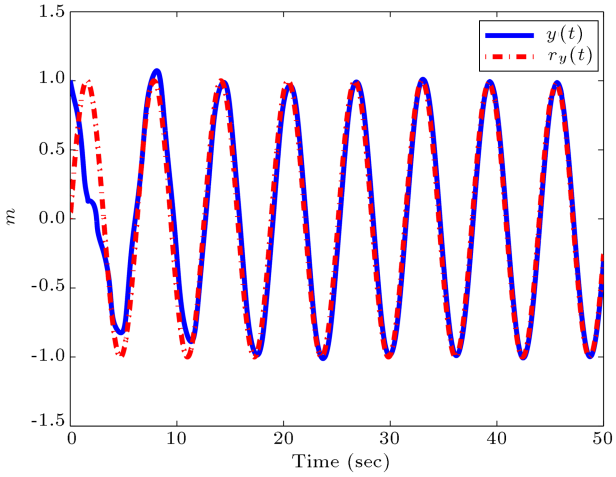

Figure 4. $y(t)$ position of the system and its reference signal $r_y(t)$. It is observed that after less than 4 second $y(t)$ converges to $r_y(t)$.

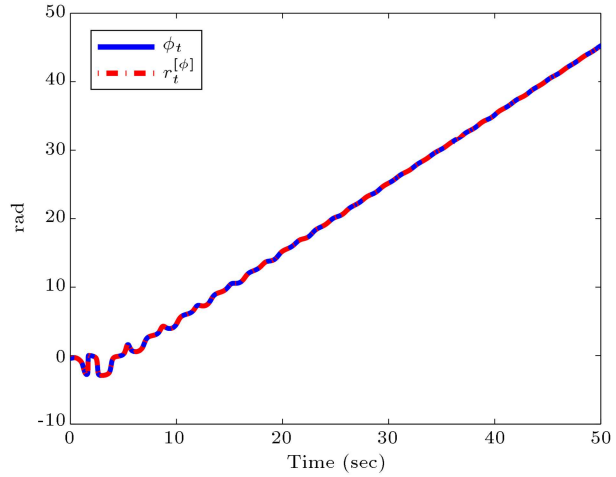

Figure 5. The heading angle of the system $\phi(t)$ and its reference signal $r_\phi(t)$. It is observed that $\phi(t)$ converges to $r_\phi(t)$ immediately.

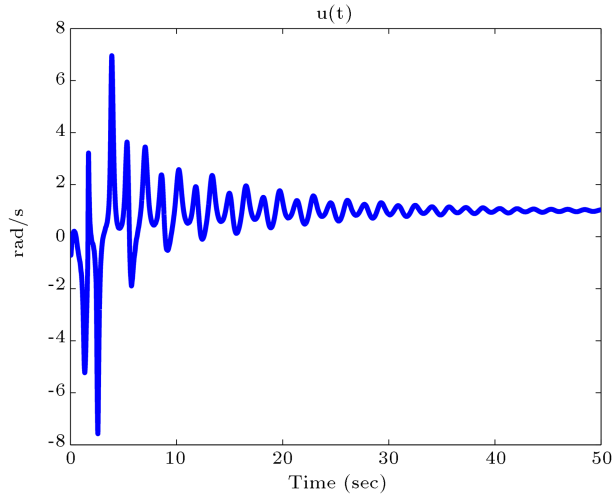

Figure 6. The control signal input to the system, which determines the angular velocity.

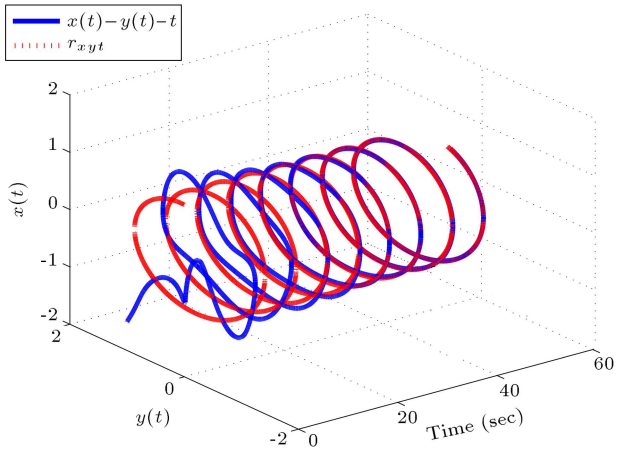

Figure 7. $x(t) - y(t) -$ time diagram

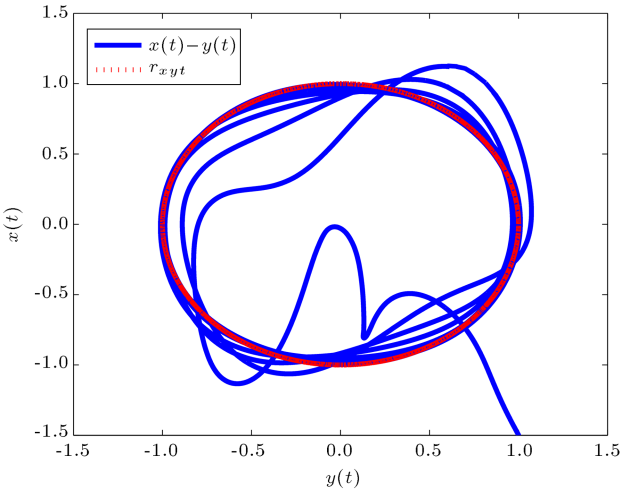

Figure 8. $x(t) - y(t)$ diagram

Table 1. Root Cumulative Square Error (RCSE) vs ω.

ω	RCSE
0.2	7.91
1	5.53
10	5.59
100	5.48
1000	5.45

feedback linearization control technique of [35] (with the linearized system of (9) and (10) of [35]) to the block diagram of Figure 1 for the reference signals of $r_x(t) = 0.0005t$ and $r_y(t) = 0.0002t$. The RCSE computed for the period of [20, 50] second when the proposed technique is used is 5.43 (see Figure 9) and the RCSE computed for the feedback linearization control technique of [35] is 17.36 (see Figure 10). From these figures, it is clear that the proposed technique has a better performance in the presence of communication imperfections.

Over the packet erasure channel, which is subject

to random packet dropout and quantization imperfections, [36] presented a novel technique, which is based on the linearization method, for the reference tracking of the unicycle model of (1). Comparison of the simulation results of this section with those of [36] for tracking a circle reveals that the approximate method presented in this paper for the unicycle model is as good as the linearization method used in [36].

Remark 6.1. i) Simulation studies illustrate that the linear approximation method proposed in this paper which is based on the describing function is good for the particular nonlinear system considered in this paper. Although the describing function is obtained for a sinusoidal input, from Figure 6, it is clear that for the non-sinusoidal inputs, the approximation must be also good. Otherwise, we did not get such a good reference tracking as well as state tracking of the nonlinear system (in Figures 3–5, 7, 8) for an estimator and controller which are based on the approximate linear system. ii) In order to utilize the communication channel and transmit a signal with the maximum allowable powers, Po_i $(i = 1, 2)$, the encoder gain $C(t)$ is computed in Propositions 4.1 – 4.3 so that:

$$\Big[var[C(t)(X(t) - \hat{X}(t))]\Big]_{ii} = Po_i.$$

However, by using the proposed coding scheme and as $P(t) \to \underline{0}$, some elements of the matrix gain $C(t)$ tend to infinity. To avoid this situation, the following modifications in the encoder matrix gain $C(t)$ are suggested:

- For the encoder matrix gain of Proposition 4.1 when $p_{ii}(t) < 0.01\gamma_1\tilde{r}_i$, we replace $p_{ii}(t)$ in the matrix gain $C(t)$ by $p_{ii}(t) + 0.01\gamma_1\tilde{r}_i$;
- For the encoder matrix gain of Proposition 4.3, when $p_{ii}(t) < 0.01Po_i\tilde{r}_i$, we replace $p_{ii}(t)$ in the matrix gain $C(t)$ by $p_{ii}(t) + 0.01Po_i\tilde{r}_i$;
- For the encoder matrix gain of Proposition 4.2, let $h = \min(\frac{\delta\tilde{r}_1}{2}, \frac{\tilde{r}_2}{2\delta})$; when $p_{ii}(t) < 0.01h$, we replace $p_{ii}(t)$ in the matrix gain $C(t)$ by $p_{ii}(t) + 0.01h$.

Using the above modifications, when $P(t) \to \underline{0}$, the elements of the matrix gain $C(t)$ remain bounded. We repeated computer simulation for $\omega = 1$, $\omega_r = 1$ and tracking the circle using the modified encoder matrix gain; and we observed that given the expense of transmission with the power a bit less than the maximum allowable power, we get RCSE = 5.55 which is very close to the RCSE of the corresponding case with infinite gain.

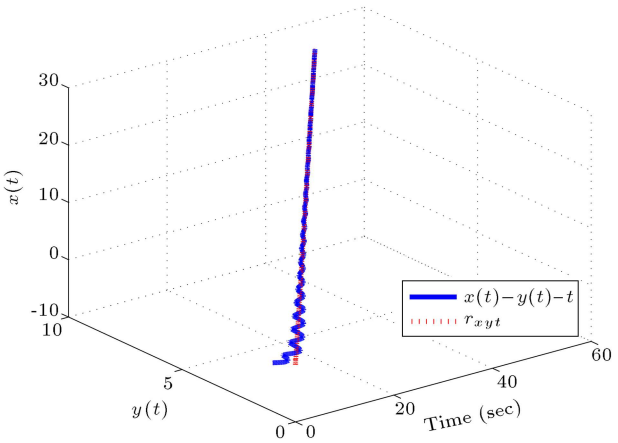

Figure 9. $x(t) - y(t) -$ time diagram for the proposed technique

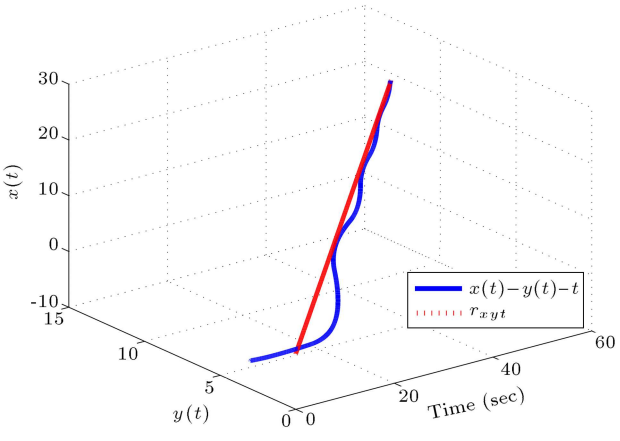

Figure 10. $x(t) - y(t) -$ time diagram for the feedback linearization technique of [35].

7. Conclusion and direction for future research

In this paper, a new technique for mean square asymptotic state tracking and reference tracking of the autonomous vehicles over analog Additive White Gaussian Noise (AWGN) channel was presented. Autonomous vehicle was cascaded with a bandpass filter acting as encoder; and hence, an approximate linear dynamic system was extracted using the describing function method. Then, the results of [13] were extended to account for systems with multiple real and non-real valued eigenvalues over Multi-Input Multi-Output (MIMO) parallel AWGN channel. Subsequently, by applying the extended results on the describing function, a technique for mean square asymptotic state tracking and reference tracking of autonomous vehicles was presented. Finally, the satisfactory performance of the proposed technique was illustrated using computer simulations.

In addition to the describing function method, there are other methods, e.g., based on the Volterra series theorem [37–39] for nonlinear analysis in the frequency domain. Using the Volterra series expansion, the Generalized Frequency Response Function (GFRF)

was defined in [40], which is multivariate Fourier transform of the Volterra kernels. This provides a useful concept for approximation of the nonlinear systems. Therefore, for future, it is interesting to compare the performance of the proposed technique with those of other approximation methods (e.g., GFRF). In addition, it is interesting to consider a more realistic model for the dynamic system (1), e.g., a dynamic system subject to measurement and process noises. This research direction is currently under investigation in our research team.

References

1. Elia, N. "When Bode meets Shannon: Control-oriented feedback communication schemes", *IEEE Trans. Automat. Contr.*, **49**(9), pp. 1477–1488 (2004).
2. Zhan, X., Guan, Z., Zhang, X., and Yuan, F. "Best tracking performance of networked control systems based on communication constraints", *Asian Journal of Control*, **16**(4), pp. 1155–1163 (2014).
3. Zhan, X., Guan, Z., Zhang, X., and Yuan, F. "Optimal tracking performance and design of networked control systems with packet dropout", *Journal of the Franklin Institute*, **350**(10), pp. 3205–3216 (2013).
4. Zhan, X.S., Wu, J., Jiang, T., and Jiang, X.W. "Optimal performance of networked control systems under the packet dropout and channel noise", *ISA Trans.*, **58**, pp. 214–221 (2015). https://doi.org/10.1016/j.isatra.2015.05.012
5. Diwadkar, A. and Vaidya, U. "Limitation for nonlinear observation over erasure channel", *IEEE Transactions on Automatic Control*, **58**(2), p. 454–459 (2013).
6. Quevedo, D.E. and Jurado, I. "Stability of sequence-based control with random delays and dropouts", *IEEE Transactions on Automatic Control*, **59**(5), pp. 1296–1302 (2014). DOI: 10.1109/TAC.2013.2286911
7. Martins, N.C., Dahleh, A., and Elia, N. "Feedback stabilization of uncertain systems in the presence of a direct link", *IEEE Trans. Automat. Contr.*, **51**(3), pp. 438–447 (2006).
8. Minero, P., Coviello, L., and Franceschetti, M. "Stabilization over Markov feedback channels: The general case", *IEEE Trans. Automat. Contr.*, **58**(2), pp. 349–362 (2013).
9. Nair, G.N., Evans, R.J., Mareels, I.M.Y., and Moran, W. "Topological feedback entropy and nonlinear stabilization", *IEEE Trans. Automat. Contr.*, **49**(9), pp. 1585–1597 (2004).
10. Nair, G.N. and Evans, R.J. "Stabilizability of stochastic linear systems with finite feedback data rates", *SIAM J. Control Optimization*, **43**(3), pp. 413–436 (2004).
11. Tatikonda, S. and Mitter, S. "Control under communication constraints", *IEEE Trans. Automat. Contr.*, **49**(7), pp. 1056–1068 (2004).
12. Charalambous, C.D. and Farhadi, A. "LQG optimality and separation principle for general discrete time partially observed stochastic systems over finite capacity communication channels", *Automatica*, **44**(12), pp. 3181–3188 (2008).
13. Charalambous, C.D., Farhadi, A., and Denic, S.Z. "Control of continuous-time linear Gaussian systems over additive Gaussian wireless fading channels: A separation principle", *IEEE Trans. Automat. Contr.*, **53**(4), pp. 1013–1019 (2008).
14. Farhadi, A. "Stability of linear dynamics systems over the packet erasure channel: A co-design approach", *International Journal of Control*, **88**(12), pp. 2488–2498 (2015).
15. Farhadi, A. "Feedback channel in linear noiseless dynamics systems controlled over the packet erasure network", *International Journal of Control*, **88**(8), pp. 1490–1503 (2015).
16. Farhadi, A., Domun, J., and Canudas de Wit, C. "A supervisory control policy over an acoustic communication network", *International Journal of Control*, **88**(5), pp. 946–958 (2015).
17. Minero, P., Franceschetti, M., Dey, S., and Nair, G.N. "Data rate theorem for stabilization over time-varying feedback channels", *IEEE Trans. Automat. Contr.*, **54**(2), pp. 243–255 (2009).
18. Zaidi, A.A., Oechtering, T.J., and Yuksel, S. "Stabilization of linear systems over Gaussian networks", *IEEE Trans. Automat. Contr.*, **59**(9), pp. 2369–2384 (2014).
19. Zaidi, A.A., Yuksel, S., Oechtering, T.J., and Skoglund, M. "On the tightness of linear policies for stabilization of linear systems over Gaussian networks", *Systems and Control Letters*, **88**, pp. 32–38 (2016).
20. Elia, N. and Eisenbeis, J.N. "Limitations of linear control over packet drop networks", *IEEE Trans. Automat. Contr.*, **56**(4), pp. 826–841 (2011).
21. Canudas de Wit, C., Gomez-Estern, F., and Rodrigues Rubio, F. "Delta-modulation coding redesign for feedback-controlled systems", *IEEE Trans. on Industrial Electronics*, **56**(7), pp. 2684–2696 (2009).
22. Braslavsky, J.H., Middleton, R.H., and Freudenberg, J.S. "Feedback stabilisation over signal-to-noise ratio constrained channels", *IEEE Trans. Automat. Contr.*, **52**(8), pp. 1391–1403 (2007).
23. Sanjeroon, V., Farhadi, A., Motahari, A., and Khalaj, B.H. "Estimation of nonlinear dynamic systems over communication channels", *IEEE Transactions on Automatic Control*, **63**(9), pp. 3024–3031 (2018).
24. Sanjeroon, V., Farhadi, A., Khalaj, B., and Motahari, A. "Estimation and stability over AWGN channel in the presence of fading, noisy feedback channel and different sample rates", *Systems and Control Letters*, **123**, pp. 75–84 (2019).
25. Farhadi, A. and Ahmed, N.U. "Suboptimal decentralized control over noisy communication channels", *Systems and Control Letters*, **60**, pp. 282–293 (2011).

26. Farhadi, A. and Charalambous, C.D. "Stability and reliable data reconstruction of uncertain dynamics systems over finite capacity channels", *Automatica*, **46**(5), pp. 889–896 (2010).
27. Farhadi, A. "Sub-optimal control over AWGN communication network", *European Journal of Control*, **37**, pp. 27–33 (2017).
28. Li, Y., Chen, J., Tuncel, E., and Su, W. "MIMO control over additive white noise channels: Stabilization and tracking by LTI controllers", *IEEE Trans. Automat. Contr.*, **61**(5), pp. 1281–1296 (2016).
29. Parsa, A. and Farhadi, A. "Reference tracking of nonlinear dynamic systems over AWGN channel using describing function", *Scientia Iranica*, **26**(3), pp. 1727–1735 (2019).
30. Liang, X. and Xu, J. "Control for networked control systems with remote and local controllers over unreliable communication channel", *Automatica*, **98**, pp. 86–94 (2018).
31. Imer, O.C., Yuksel, S., and Basar, T. "Optimal control of LTI systems over unreliable communication link", *Automatica*, **42**(9), pp. 1429–1439 (2006).
32. Slotine, J.J. and Li, W., *Applied Nonlinear Control*, Prentice-Hall (1991).
33. Kwakernaak, H. and Sivan, P., *Linear Optimal Control Systems*, Wiley-Interscience (1972).
34. Canudas de Wit, C., Sicilian, B., and Bastin, G., *Theory of Robot Control*, Springer - Verlag (1996).
35. Oriolo, G., De Luca, A., and Vendittelli, M. "WMR control via dynamic feedback linearization: Design, implementation, and experimental validation", *IEEE Trans. on Control Systems Technology*, **10**(6), pp. 835–852 (2002).
36. Parsa, A. and Farhadi, A. "Measurement and control of nonlinear dynamic systems over the Internet (IoT): Applications in remote control of autonomous vehicles", *Automatica*, **95**, pp. 93–103 (2018).
37. Jing, X. and Lang, Z., *Frequency Domain Analysis and Design of Nonlinear Systems Based on Volterra Series Wxpansion - A Parametric Characteristic Approach*, Springer International Publishing Switzerland (2015).
38. Rugh, W.J., *Nonlinear System Theory: The Volterra/Wiener Approach*, Baltimore, MD: The Johns Hopkins Univ. Press (1981).
39. Worden, K. and Tomlinson, G.R., *Nonlinearity In Structural Dynamics: Detection, Identification And Modeling*, Bristol, U.K.: Institute of Physics (2001).
40. George, D.A., *Continuous Nonlinear Systems*, MIT Research Lab. Electronics, Cambridge, MA, Tech. Rep. 355 (1959).

Biographies

Ali Parsa received his BSc and MSc degrees in Electrical Engineering from the University of Tehran, Iran in 2011 and 2014, respectively. He designed and implemented several systems and devices in the field of Smart Grid and Smart Home in the Mechatronics Lab. of the University of Tehran. He received the PhD degree from the Department of Electrical Engineering at Sharif University of Technology, Iran in 2018. His PhD research was concerned with theoretical aspects of remote estimation and control of nonlinear systems over communication channels subject to imperfections (wireless, WiFi, and the Internet) with applications in telemetry and tele-operation of autonomous vehicles. Also, he has worked at the Department of Research and Development of Crouse Co., which is the largest automotive part manufacturer in Iran, for 3 years. Currently, he is a postdoctoral researcher at the HiPeRT Lab. of the University of Modena and Reggio Emilia (UNIMORE), Modena, Italy. His main research areas include networked control systems, autonomous vehicles, automotive, Internet of Things (IoT), and smart home.

Alireza Farhadi received PhD degree in Electrical Engineering from the University of Ottawa, Ontario, Canada in 2007. After receiving PhD degree, Dr. Farhadi worked as a Postdoctoral Fellow at the Department of Electrical Engineering at the University of Ottawa (2008–2009) and the French National Institute for Research in Computer Science and Control (INRIA), Grenoble, France (2010–2011). He then worked as a Research Fellow (academic level B4) at the Department of Electrical Engineering of the University of Melbourne, Australia (2011–2013). In September 2013, he joined the Department of Electrical Engineering of Sharif University of Technology as Assistant Professor. Currently, he is an Associate Professor at the Department of Electrical Engineering of Sharif University of Technology. Dr. Farhadi specializes in the design, optimization and control of large-scale and distributed Mechatronics systems and networks with a particular focus on automated irrigation network, intelligent inspection and fault diagnosis systems, smart oil field, fleets of autonomous under water, unmanned aerial and autonomous road vehicles, smart building, IIOT, industry 4.0 and intelligent embedded systems.